

Transient rheological probing of PIB/hectorite-nanocomposites

Jun Hee Sung^{1,2}, Jan Mewis^{1*} and Paula Moldenaers¹

¹Department of Chemical Engineering, Katholieke Universiteit Leuven, W. de Croijlaan 46,
B-3001 Leuven (Heverlee), Belgium

²Department of Chemical and Biological Engineering, Applied Rheology Center, Korea University, Seoul, 136-701, Korea.

(Received Dec. 4, 2007; final revision received Jan. 23, 2008)

Abstract

Clay suspensions in liquid polymers exhibit a time-dependent behaviour that includes viscoelastic as well as thixotropic features. Because of the presence of interacting clay platelets, particulate networks can develop, which are broken down during flow and rebuild upon cessation of the flow. Here, the use of thixotropic techniques in probing flow-induced structures in nanocomposites is explored with data on a hectorite-poly(isobutylene) model system. By means of fast stress jump measurements the hydrodynamic contributions to the steady state stresses are determined as well as those caused by the stretching of the clay flocs. Flow reversal measurements do not provide a clear indication of flow-induced anisotropy in the present case. The recovery of the clay microstructure upon cessation of flow is followed by means of overshoot and dynamic measurements. The development of a particulate network is detected by the appearance and growth of a low frequency plateau of the storage moduli. The modulus-frequency curves after various rest times collapse onto universal master curves, regardless of the pre-shear history or temperature. The scaling factors for this master curve are the crossover parameters. The crossover moduli are nearly a linear function of the crossover frequency, the relation being identical for recovery after shearing at different shear rates. This function depends, however, on temperature.

Keywords : clay suspension, nanocomposite, thixotropy, stress jumps, scaling function

1. Introduction

The success of polymer/clay nanocomposites is based on the high performance that can be achieved via nanoscale reinforcement using highly anisotropic layered silicates (Giannelis, 1996; Giannelis *et al.*, 1999; Ray and Okamoto, 2003). Particle size and shape, surface morphology, and distribution within the polymeric matrix are all important parameters in this context. A substantial reinforcement requires compatibility between the inorganic material and the polymer. Inorganic fillers have traditionally been made hydrophobic to induce compatibility with a polymer phase, this is also the case for clay particles (Ray and Okamoto, 2003; Alexandre and Dubois, 2000). Nevertheless, the interaction between a grafted or adsorbed polymer and a polymer melt matrix, as well as the ensuing steric stability of colloidal particles, is not straightforward (Green and Mewis, 2006); the presence of nanoparticles can entail additional phenomena (Mackay *et al.*, 2006).

Clays are potentially well suited for the design of hybrid composites because their lamellar elements have high in-

plane strength and a high aspect ratio. Hectorite and montmorillonite are commonly used for this purpose. Normally the clay platelets are stacked in tactoids. To achieve highly performant composites, the tactoids should be separated as far as possible in individual layers by means of intercalation and exfoliation. In the case of an intercalated state, polymer is present in the interlayer galleries but the layered structure of the silicate is maintained. In this state the stacked silicate layers, swollen by polymer, can flocculate to a certain extent. Flocculation is, however, not as extensive as in the totally exfoliated state where the clay layers are fully dispersed in the polymer matrix, providing the largest possible interfacial area. Exfoliation is not easy to achieve with polymers and several methods have been suggested for this purpose (Ray and Okamoto, 2003; Alexandre and Dubois, 2000). Solvents or in-situ polymerization facilitate the penetration of polymer in the galleries. Melt processing is the more difficult but preferred process, it has been successfully applied in various cases (Vaia and Giannelis, 1997; Kato *et al.*, 1997; Kawasumi *et al.*, 1997). The polar surface makes pure clays incompatible with polymers that have a low polarity. To improve the degree of dispersions the clay can be organically modified. Ion-exchange reactions with alkylammonium or alkylphospho-

*Corresponding author: jan.mewis@cit.kuleuven.be
© 2008 by The Korean Society of Rheology

nium surfactants are commonly used for this purpose.

In the liquid state nanocomposites basically behave as filled polymers but also display features of colloidal suspensions (Krishnamoorti and Giannelis, 1997). The latter implies that the rheological curves of nanocomposites are not merely shifted with respect to those of the suspending polymer melt as would be the case with purely hydrodynamic effects. Colloidal forces can induce additional stresses that affect mainly the low shear properties. Interparticle attraction forces cause floc formation, which is mainly responsible for the complex shear and time effects in clay/polymer systems. As in any other colloidal system, the effects of interparticle forces become more prominent with decreasing particle size (Le Meins *et al.*, 2002); improved dispersion of the particles also increases the available interface and has a similar effect on the rheology. When the flocs percolate, a space-filling particulate network is formed which causes a plateau storage modulus at low frequencies as well as a yield stress in the viscosity curve. Such a type of behaviour has often been reported for polymer/clay nanocomposites (Hoffmann *et al.*, 2000; Krishnamoorti and Yurekli, 2001).

Flow affects the microstructure of colloidal systems and this is also the case for clay/polymer nanocomposites. A change in shear rate will result in a corresponding change in the particulate structure, determined here by the floc structure and/or particle orientation. Because of the high viscosity of the suspending medium structural changes might require quite some time, and thus display thixotropic behaviour, and this at a slower rate than in most ordinary thixotropic suspensions (Solomon *et al.*, 2001; Vermant *et al.*, 2007). The possible mechanisms involved have not been completely elucidated; in particular the role of Brownian motion in structure recovery at rest is questioned (Solomon *et al.*, 2001; Lele *et al.*, 2002; Ren *et al.*, 2003). The slow kinetics make it difficult to reach the steady state during flow or equilibrium conditions at rest. Different shear histories can then result in different pseudo-equilibrium structures (Mobuchon *et al.*, 2007). It is the thixotropic aspect of clay-nanocomposites that will be considered here. Transient rheological properties of such materials will be investigated using techniques that have been applied to thixotropic suspensions in low viscosity media (Mewis, 1979; Barnes, 1997), including stress overshoot and flow reversal. The components of the steady state stresses will be analyzed using the stress jump method. Start-up flow and dynamic measurements provide means to follow structure recovery after cessation of flow. This work builds on, and extends, earlier work of Solomon *et al.* (2001), Mobuchon *et al.* (2007) and Vermant *et al.* (2007).

2. Materials and methods

As polymer matrix polyisobutylene (PIB, Parapol 1300

from ExxonMobil Chem. Co) has been selected. It is a polar and liquid at ambient temperature, and it has often been used as a model material (Grizzuti and Bifulco, 1997; Jansseune *et al.*, 2001). The sample used here has a density of 890 kg/m^3 and a viscosity of $102.5 \text{ Pa}\cdot\text{s}$ at 23°C . The clay is a refined white hectorite that has been exchanged with a dimethyldihydrogenated tallow quart (provided by Elementis Specialties). It consists of anisotropic particles of nanometer size.

A solution procedure was followed to disperse the clay in the PIB with cyclohexane as the solvent. The value of the χ parameter for the cyclohexane-PIB system is 0.57 at 25°C (Brandrup and Immergut, 1989). The clay was dispersed in the solvent using an ultrasonic generator (Elma, Transonic 700/H, Belgium); The PIB was then dissolved in the resulting clay-solvent suspension. Subsequently, the solvent was removed by evaporation at 50°C under a pressure of 10 mbar during 7~8 hours. It is well known that it is extremely difficult to eliminate all the solvent in this manner and residual solvent will be present in the sample. The focus of the present work is on the methodology and the detailed nature of the sample is not critical. The clay concentration in the final sample was 8 wt%.

The rheological measurements on the clay/polymer suspension were performed on a strain controlled device (ARES, TA Instruments) at 23°C . A cone and plate geometry (25 mm radius and 0.1 rad cone angle) ensured a constant shear history throughout the whole sample, which is essential for nonlinear transient measurements. Possible intercalation and exfoliation were evaluated with small angle x-ray scattering (SAXS). Data were recorded with a Rigaku Kratky camera on a Rigaku Rotaflex RU-200B rotating Cu anode at a power of 4 kW. The X-ray source was operated at 100 mA and 40 kV. Cu K_α radiation was obtained by filtering with Ni, and data were collected on a Braun linear position sensitive detector. The scattered

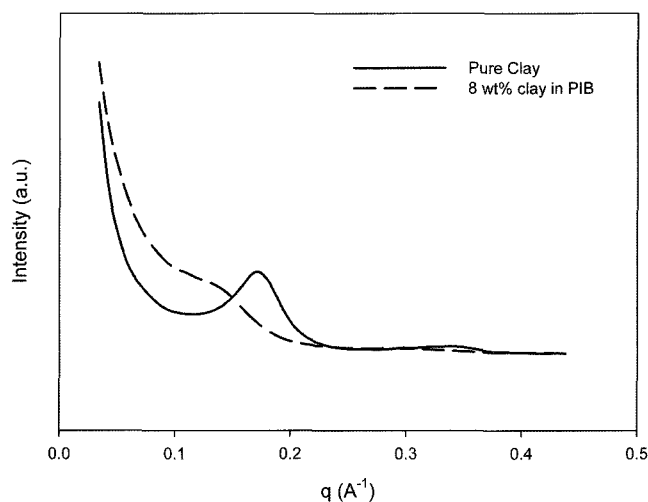


Fig. 1. SAXS patterns of pure clay and of the 8 wt% clay dispersion in PIB.

intensity was recorded during 1 hour at room temperature (23°C). The samples were placed in an aluminum holder with a thickness of about 2 mm, sealed with aluminum foil. After smoothing the data, the slit-smear intensity patterns were desmeared using the Guinier-Dumond procedure (DuMond, 1947). Intercalation of the polymer chains in the clay galleries should increase the interlayer spacing, leading to a shift of the diffraction peak.

Fig. 1 shows the recorded small angle X-ray scattering (SAXS) patterns of the pure clay and of the suspension of 8 wt% clay in the PIB matrix. The peaks are at $q=0.1753 \text{ \AA}^{-1}$ for pure clay and at $q=0.1426 \text{ \AA}^{-1}$ for the 8 wt% clay dispersion, corresponding to lattice parameters of 3.6 nm and 4.4 nm respectively, as derived from the Lorentz-corrected scattering. From the decreased peak height and the peak widening of the SAXS curves for the clay dispersed in PIB, it can be concluded that the clay is partially intercalated and partially exfoliated.

3. Results and discussion

3.1. Stress jumps

Colloidal suspensions that contain weakly attractive particles display a complex rheological behaviour. Their viscosity depends on both shear rate and time, but in a manner different from that normally seen in ordinary polymer liquids. When shearing an attractive colloidal system that has been at rest for a sufficiently long time, the viscosity decreases gradually in time. When the shear rate is subsequently reduced, the material gradually recovers its original viscosity (Mewis, 1979; Barnes 1997). This defines thixotropic behaviour, assuming the flow-induced changes are reversible. Inspired by the behaviour of glasses, such time effects are also known as *ageing* and *rejuvenation* (Bonn *et al.*, 2004; Hyunh *et al.*, 2005). The difference between the usual viscoelastic behaviour and thixotropy is most obvious in the stress response resulting from a sudden decrease in shear rate. In polymer fluids such an experiment will normally cause a linear or nonlinear stress relaxation. For thixotropic systems, however, the stress will actually increase in time because of the rebuilding of particle clusters and/or the re-orientation of anisotropic clusters or particles. In principle this increase might be preceded by a fast decrease, resulting from the relaxation of the flocs that have been stretched during shearing (Mobuchon *et al.*, 2007; Dullaert and Mewis, 2005a).

The stress response following a sudden decrease in shear rate from 5 to 0.5 s^{-1} is illustrated in Fig. 2 for the 8 wt% clay suspension. To access the short time response a suitable procedure has to be followed (Mackay *et al.*, 1992; Dullaert and Mewis, 2005b), involving the elimination of the filter on the output signal of the device and the use of a fast data acquisition system. Tests with Newtonian fluids indicate that the real material response can be detected

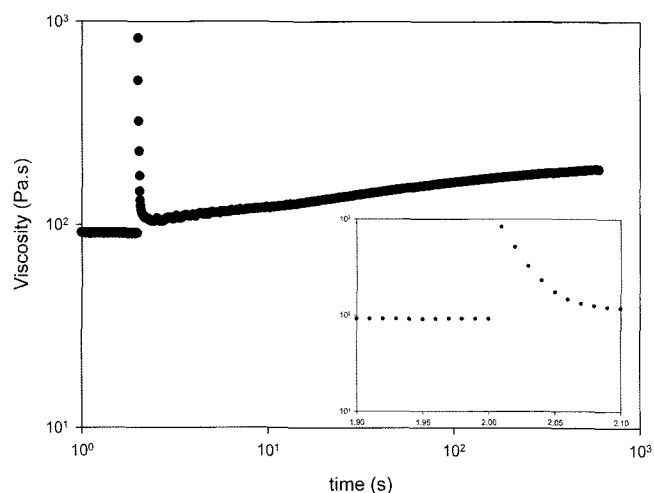


Fig. 2. Viscosity as a function of time for a 8 wt% clay suspension after a sudden drop in shear rate from 5 s^{-1} to 0.5 s^{-1} ; insert: detail of stress relaxation.

after about 30 ms (Dullaert and Mewis, 2005b). The initial relaxation in the sample, which is associated with the stresses in the polymer matrix, is actually too fast to be distinguished clearly from the dynamic response of the instrument itself. The polymer was actually selected for this reason, because the fast relaxation of the polymer itself makes it possible to detect and identify other fast relaxation mechanisms as discussed below.

Immediately after the stresses are relaxed, following a stepwise reduction in shear rate, they can be seen (Fig. 2) to start increasing again, which is a characteristic feature of thixotropic materials. In the present case the stress growth is very slow and continues for a very long time. The high viscosity of the suspending fluid probably plays a role here, although the thixotropic stress recovery can also be very slow in systems with a low viscosity matrix (Willenbacher 1996; Potanin, 2004). It then becomes difficult to determine the steady state viscosity at low shear rates.

The shear stress in complex fluids can often be decomposed in a viscous or hydrodynamic component and in a so-called “elastic” component (Batchelor, 1970). The former is directly determined by the instantaneous shear rate whereas the latter is associated with some microstructural features that take time to relax. When suddenly arresting the flow, the hydrodynamic component in a viscous medium would immediately drop to zero and therefore cause a “stress jump”. The structural contribution to the stress would gradually relax in time. This procedure has been applied on various materials, including polymer blends (Vinckier *et al.*, 1997), stable colloidal suspensions (Mackay and Kaffashi, 1995), flocculated suspensions (Dullaert and Mewis, 2005b) and recently also on clay nanocomposites (Mobuchon *et al.*, 2007).

The stress jump technique has also been applied to the clay/polymer composite under consideration to identify the

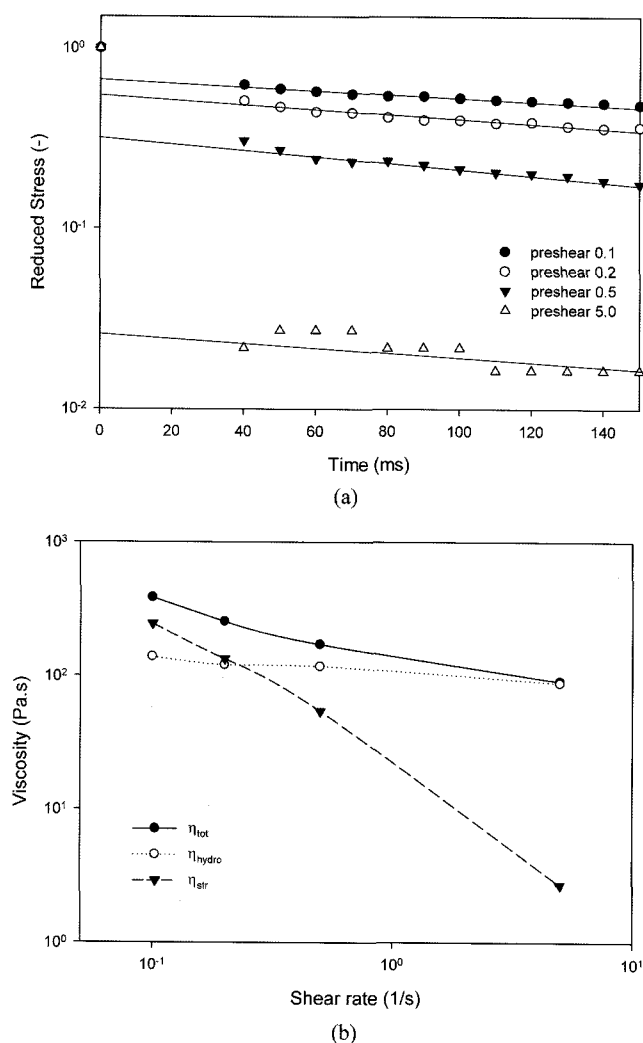


Fig. 3. (a) Stress jumps and stress relaxation after shearing at 0.1, 0.2, 0.5 and 5.0 s⁻¹; (b) hydrodynamic and structural contributions to the steady state viscosity.

stress components. Fig. 3(a) shows the initial part of the stress relaxation curves when arresting the flow after shearing at various shear rates. The stresses are reduced values, *i.e.* they are expressed as a fraction of the steady state value before cessation of flow. The measurement procedure is the same that has been followed in Fig. 2. Data collection started after the dynamic response of the instrument and the stress relaxation in the polymer had been completed. The initial stress jump, obtained by extrapolating the stress relaxation curves to time zero, measures the hydrodynamic contribution that is caused here by the flow in the polymer matrix. The initial parts of the relaxation curves are sufficiently linear in a log-linear representation to obtain reliable extrapolated values of the reduced stresses. These are 0.65, 0.53, 0.32 and 0.03 after shearing at respectively 0.1, 0.2, 0.5 and 5 s⁻¹. The remaining part of the stress, *i.e.* the part that gradually relaxes after stopping the flow, reflects the non-hydrodynamic stress contributed by the particulate

clay structure. This part of the stress dominates at low shear rates and should constitute nearly the total stress when the dynamic yield stress is reached (Mobuchon *et al.*, 2007; Dullaert and Mewis, 2005b).

Fig. 3(b) shows the decomposition in terms of total viscosity η_{tot} . The hydrodynamic part η_{hydro} changes relatively little over the range of shear rates covered here, *i.e.* less than 50%. On the other hand, the “elastic” or structural contribution to the viscosity, η_{str} drops by two orders of magnitude. It systematically disappears at higher shear rates, contributing about 3% of the stress during flow at 5.0 s⁻¹. This difference is in line with earlier results on weakly flocculated dispersions (Dullaert and Mewis, 2005b), where the flow caused a gradual breakdown of the flocs. This breakdown causes a reduction of the hydrodynamic resistance as well as of the elastic stress that can be stored in the deformed flocs. The relaxation time of the hydrodynamic part does not change much with shear rate, similar to what has been reported for normal flocculated colloidal suspensions (Dullaert and Mewis, 2005b).

3.2. Flow Reversals

Flow reversal experiments can provide information about the anisotropy of the particulate structure with respect to the plane perpendicular to the velocity direction. If there are no relaxational phenomena involved, the initial stress after a rapid flow reversal should be the hydrodynamic stress of the objects in their original orientation or deformation but with the flow in the opposite direction because the particulate structure cannot change instantaneously. Subsequently, it will gradually adapt to the new flow direction, either by deformation, rotation or repositioning, depending on the nature of the structure. After the reorientation is completed, the magnitude of the stress should equal the original value before flow reversal, but now in the opposite direction. This technique has been applied to demonstrate flow-induced anisotropy in structured polymers, such as liquid crystalline polymers and immiscible polymer blends (Moldenaers *et al.*, 1989; Minale *et al.*, 1999), as well as in suspensions of particles (Gadala-Maria and Acrivos, 1980). With this procedure, the anisotropy of weakly aggregated flocs has also been demonstrated (Dullaert and Mewis, 2008).

Fig. 4(a) shows the results of flow reversal experiments on the 8 wt% clay dispersion in PIB at different shear rate levels between 0.1 and 5.0 s⁻¹. As in the stress jump experiments, the polymer matrix relaxes before the first data points are recorded after 30 ms. With a maximum shear rate of 5 s⁻¹ the applied strain after 30 ms is at most 0.15. Such a small value precludes a significant rotation of any anisotropic structural element that might be present. In the absence of structural stress components an extrapolation of the stress curves to time zero, *i.e.* the time of flow reversal, could then provide an indication of anisotropy. The stress

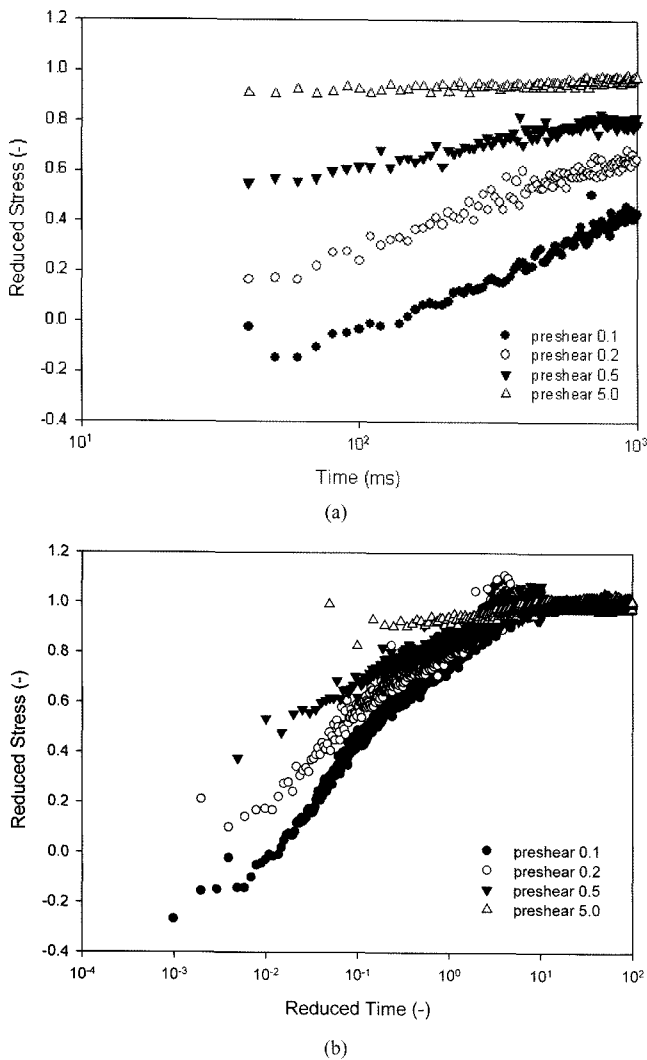


Fig. 4. (a) Flow reversal experiments at different pre-shear rates, stresses are reduced by the steady state value; (b) reduced stress vs. reduced time ($\dot{\gamma} \cdot t$) for the same experiments.

values immediately before and after flow reversal should then differ by the sum of the hydrodynamic stress components in the forward and the reverse directions. In case of anisotropy the reverse one could differ from the forward one and hence the total stress jump should not equal twice the value that has been determined in the stress jump experiments of Fig. 3. With the present system the structural stress should be considered as well. It relaxes, however, quite slowly: approximately 1.5% of the initial value after 30 ms. This relaxation, increased by a stretching of the structure in the opposite direction should be added to the sum of the hydrodynamic stresses but this would be a rather small correction in the present case. Applying this procedure to the data of Fig. 4, with the hydrodynamic stress components given above for the stress jumps, fits the experimental data quite well. Hence, it must be concluded that the initial response to the flow reversal does not sug-

gest any significant degree of anisotropy in the present system.

Also the stress evolution resulting from flow reversal should reflect whatever anisotropy the system displays, as it should track the reorientation of the structural elements towards the reverse direction. The tumbling of a rigid, non-Brownian object would produce a stress pattern that is strain controlled, meaning that results for different shear rates would superimpose when the time is scaled with the shear rate. Such scaling has also been reported for flow-induced clusters and reversible aggregates of spherical particles (Gadala-Maria and Acrivos, 1980; Dullaert and Mewis, 2008). It does, however, not apply in the present case, as can be seen in Fig. 4(b). Even using a reduced time scale, *i.e.* comparing the curves at similar strain levels, a higher shear rate results in a faster relaxation. The scaling cannot be expected to hold in general for reversible aggregates as the aggregate structure can change with shear rate. Yet, the stress transients should still reflect the reorientation of the anisotropic flocs. However, from the stress jump experiments (Fig. 3) it is known that the clay flocs relax, this happens over the same time range as the stress transients in flow reversals. Because of the interference of floc relaxation and stretching, it is impossible to detect any systematic feature in the stress curves that could be univocally associated with anisotropy. This lack of clear signs of anisotropy is consistent with the data for the initial stress values after reversing the flow. It must be concluded that the present system has at most only a limited degree of anisotropy, which is too small to be detected by simple flow reversal experiments.

3.3. Thixotropic recovery at rest

Structural recovery after cessation of flow can be probed by means of destructive and non-destructive techniques. The former are illustrated by the use of intermittent flows. When the flow is started up again after a given period of rest, the start-up stress curve is measured and the overshoot stress is recorded. The evolution of the overshoot stress with rest time can be used to characterize the thixotropic recovery at rest. This is illustrated for the system under consideration in Fig. 5. It is obvious that the structure strengthens very gradually and that reaching the ultimate overshoot stress will take very long rest times. The peak strain remains rather constant during this stage of the structure recovery and is of order unity. This is a very large value for a flocculated suspension but clay nanocomposites can show quite high values (Solomon *et al.*, 2001; Vermant *et al.*, 2007), although this is not necessarily the case for clay dispersions in low viscosity media (Pignon *et al.*, 1998).

Dynamic moduli provide an alternative, non-destructive technique to follow structural recovery at rest. This technique also provides linear viscoelastic information about

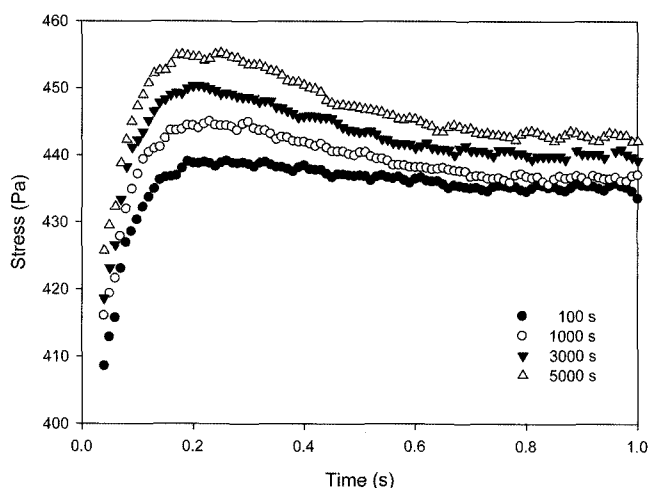


Fig. 5. Start-up curves for intermittent shear flow at 5 s^{-1} and different rest periods.

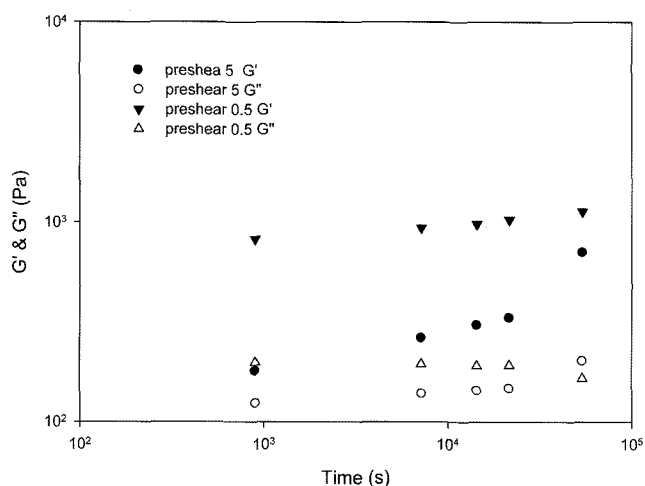


Fig. 6. Evolution of the linear dynamic moduli at 0.3 rad/s after shearing at 0.5 and 5 s^{-1} ($T=23^\circ\text{C}$).

the existing microstructure. Fig. 6 shows the initial evolution of the dynamic moduli, G' and G'' , for two different shear histories at a temperature of 23°C . The measurements have been performed at a low frequency, 0.3 rad/s , in order to achieve a high degree of sensitivity to structural changes. The peak strain (0.01) is sufficiently low to ensure the data to be within the linear region. During shear flow at 0.5 s^{-1} a particulate structure remains present that is capable of bearing a substantial elastic stress, as was demonstrated by the stress jump measurements (Fig. 3). Hence, it is not surprising that the storage moduli dominate the loss moduli after arresting the flow. On the other hand, by shearing at 5 s^{-1} the particulate structure is nearly completely broken down (Fig. 3), resulting in much lower moduli.

As is common in thixotropic suspensions, the elastic part grows more and faster at rest, as it is more sensitive to structural changes than the loss modulus, again in line with the results of the stress jump experiments of Fig. 3. The

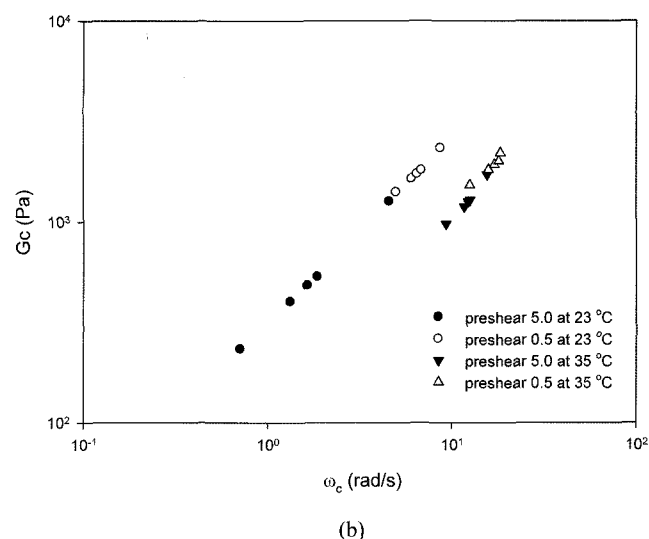
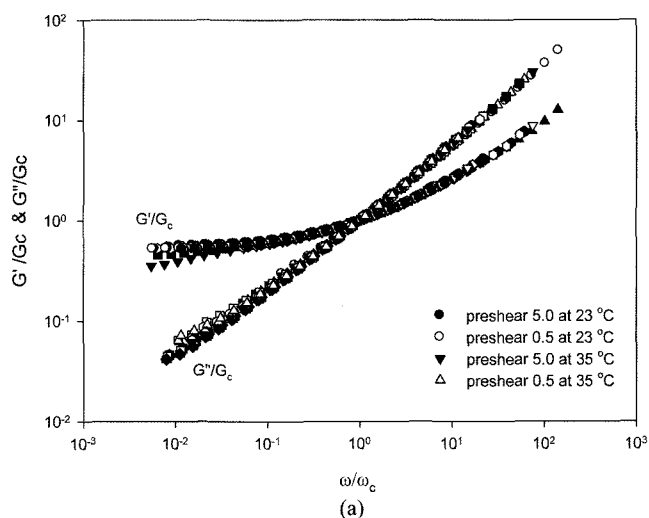


Fig. 7. (a) Master curves for the dynamic moduli at various rest times (between 2 and 24 hrs) after shearing at 0.5 and 5 s^{-1} at 23 and 35°C ; (b) scaling parameters for the scaling of (a).

mechanisms that govern the structural growth in clay/polymer nanocomposites at rest are not elucidated yet, in particular the role of Brownian motion and particle rotation have been questioned (Solomon *et al.*, 2001; Ren *et al.*, 2003). The changes in Fig. 6, as those in Fig. 3, are consistent with results on weakly flocculated thixotropic suspensions: higher shear rates result in smaller aggregates that grow faster in time. It should be pointed out that the structure that develops from the smallest aggregates, *i.e.* here after shearing at 5 s^{-1} , does not necessarily recover the same intermediate microstructures as are being generated when the sample has been sheared at 0.5 s^{-1} . In each case a fractal-like structure might develop but the building blocks, *i.e.* the aggregates resulting from the earlier shear flow, are different. The difference can be demonstrated by rheological and other techniques (Mewis *et al.*, 1975; Wyss

et al., 2005).

After a sufficiently long rest period the rate of change for the moduli slows down and it becomes possible to record the moduli-frequency curves as a function of time. The frequency dependence of the high frequency data corresponds to those of the polymer matrix, with a relatively small increase of the moduli due to the presence of solid inclusions. The low frequency moduli, especially the storage moduli, increase much more and develop a plateau that reflects the development of a percolating network of flocs. As a result of the faster growth of the low frequency storage moduli the crossover point ($G' = G''$) of the G' and G'' curves gradually shifts to higher frequencies. Weitz and collaborators (Trappe and Weitz, 2000; Prasad *et al.*, 2003) have suggested a universal behaviour for the liquid-solid transition in dispersions of attractive particles. This involves a similarity in the moduli-frequency curves for systems in which the particle volume fraction or the strength of interparticle attraction force is systematically increased to induce the transition. The various sets of curves for G' and G'' can then be superimposed by a scaling procedure, in which the crossover modulus and frequency, $G'_c = G''_c$ and ω_c , are used as scaling factors. In Fig. 7(a), this scaling has been applied to the time-dependent moduli-frequency curves of the system under consideration, and this for recovery after shearing at 0.5 and 5 s⁻¹ at 23 and 35°C.

Clearly, the scaling procedure seems to apply to the present data, providing a single master curve for different shear histories and temperatures. The physical meaning of this scaling could perhaps be questioned because the shape of the curves is bound to be very similar in all cases. For instance, all G' curves have a low frequency plateau, and the limiting high frequency behaviour of both moduli is that of the matrix polymer. The nature of the scaling parameters has been considered in more detail. The relation between G_c and ω_c for two different preconditioning shear rates and two temperatures is shown in Fig. 7(b). The absolute values of the scaling parameters depend on the previous shear rate but the data for the two different shear histories are on the same line. This is the case for the two different temperatures used, but the change in temperature caused a parallel shift of the line.

Conclusions

Clay/polymer nanocomposites display thixotropic features, they can be studied by means of transient rheological measurements. Using fast stress jump experiments, stresses during shear flow have been decomposed in direct hydrodynamic and structural contributions. The main source of shear thinning is of structural rather than of purely hydrodynamic origin. The stress transients resulting from flow reversals do not provide a clear indication of flow-induced anisotropy in the present system. A low frequency plateau

develops in the time-dependent moduli-frequency curves that are obtained after cessation of flow, as observed earlier in various systems. The time-dependent moduli obey a scaling that has been suggested by Weitz *et al.* (Trappe and Weitz, 2000; Prasad *et al.*, 2003) for weakly flocculated suspensions. Using the parameters of the crossover point as scaling factors, the curves of storage and loss moduli versus frequency at various times collapse on master curves. The relation between crossover moduli and crossover frequencies was found to be independent of shear history. Changing the temperature resulted in a parallel shift of that relation.

Acknowledgements

J. H. Sung gratefully acknowledges support from the Korea Science and Engineering Foundation (KOSEF) through the Applied Rheology Center (ARC) at Korea University, Korea. Dr. W. Ijdo and Elementis-Specialties provided the hectorite sample. Dr. B. Goderis (K.U.Leuven) is thanked for making the X-ray measurements possible.

References

- Alexandre, M. and P. Dubois, 2000, Polymer-layered silicate nanocomposites: preparation, properties and used of a new class of materials, *Mater. Sci. Eng.* **28**, 1-63.
- Barnes, H. A., 1997, Thixotropy- A review, *J. Non-Newtonian Fluid Mech.* **70**, 1-33.
- Batchelor, G. K., 1970, The stress system in a suspension of force-free particles, *J. Fluid Mech.* **41**, 545-570.
- Bonn, D., H. Tanaka, P. Coussot and J. Meunier, 2004, Ageing, shear rejuvenation and avalanches in soft glassy materials, *J. Phys.: Condens. Matter* **16**, S4987-S4992.
- Brandrup, J. and E. H. Immergut, 1989, Polymer Handbook 3rd, *John Wiley and Sons*, VII/175.
- Dullaert, K. and J. Mewis, 2005a, Thixotropy: build-up and breakdown curves during flow, *J. Rheol.* **49**, 1213-1230.
- Dullaert, K. and J. Mewis, 2005b, Stress jumps on weakly flocculated dispersions: steady state and transient results, *J. Colloid Interface Sci.* **287**, 542-551.
- Dullaert, K. and J. Mewis, 2008, to be published.
- DuMond, J. W. M., 1947, Method of correcting low angle X-Ray diffraction curves for the study of small particle sizes, *Phys. Rev.* **72**, 83-84.
- Gadala-Maria, F. and A. Acrivos, 1980, Shear-induced structure in a concentrated suspension of solid spheres, *J. Rheol.* **24**, 799-814.
- Giannelis, E. P., R. Krishnamoorti and E. Manias, 1999, Polymer-silicate nanocomposites: model system for confined polymers and polymer brushes, *Advances Polym. Sci.* **138**, 107-147.
- Giannelis, E. P. 1996, Polymer layered silicate nanocomposite, *Adv. Mater.* **8**, 29-35.
- Green, D. L. and J. Mewis, 2006, Connecting the wetting and rheo-

- logical behaviours of poly(dimethylsiloxane)-grafted silica spheres in poly(dimethylsiloxane) melts, *Langmuir* **22**, 9546-9553.
- Grizzuti, N. and O. Bifulco, 1997, Effect of coalescence and breakup on the steady-state morphology of an immiscible polymer blend in shear flow, *Rheol. Acta* **36**, 406-415.
- Hoffmann, B., C. Dietrich, R. Thomann, C. Friedrich and R. Mulhaupt, 2000, Morphology and rheology of polystyrene nanocomposites based upon organoclay, *Macromol. Rapid Comm.* **21**, 57-61.
- Hyunh, H. T., N. Roussel and P. Coussot, 2005, Aging and free surface flow of a thixotropic fluid, *Phys. Fluids* **17**, 033101-033101-9.
- Jansseune, T., I. Vinckier, P. Moldenaers and J. Mewis, 2001, Transient stresses in immiscible model polymer blends during start-up flow, *J. Non-Newtonian Fluid Mech.* **99**, 167-181.
- Kato, M., A. Usuki and A. Okada, 1997, Synthesis of polypropylene oligomer-clay intercalation compounds, *J. Appl. Polym. Sci.* **66**, 1781-1785.
- Kawasumi, M., N. Hasegawa, M. Kato, A. Usuki and A. Okada, 1997, Preparation and mechanical properties of polypropylene-clay hybrids, *Macromolecules* **30**, 6333-6338.
- Krishnamoorti, R. and E. Giannelis, 1997, Rheology of end-tethered polymer layered silicate nanocomposites, *Macromolecules* **30**, 4097-4102.
- Krishnamoorti, R. and K. Yurekli, 2001, Rheology of polymer layered silicate nanocomposites, *Curr. Opin. Colloid Interface Sci.* **64**, 464-470.
- Le Meins, J-F., P. Moldenaers and J. Mewis, 2002, Suspensions in polymer melts, 1. effect of particle size on the shear flow behaviour, *Ind. Eng. Chem. Res.* **41**, 6297-6304.
- Lele, A., M. Mackley, C. Ramesh and G. Galgali, 2002, In situ rheo-x-ray investigation of flow-induced orientation in layered silicate-syndiotactic polypropylene nanocomposites melt, *J. Rheol.* **46**, 1091-1110.
- Mackay, M. E. and B. Kaffashi, 1995, Stress jumps of charged colloidal suspensions, measurement of the elastic-like and viscous stress components, *J. Colloid Interface Sci.* **174**, 117-123.
- Mackay, M. E., A. Tuteja, P. M. Duxbury, C. J. Hawker, B. Van Horn, Z. Guan, G. Chen and R. S. Krishnan, 2006, General strategies for nanoparticle dispersion, *Science* **311**, 1740-1743.
- Mackay, M. E., C. H. Liang and P. J. Halley, 1992, Instrument effects on stress jump measurements, *Rheol. Acta* **31**, 481-489.
- Mewis, J., 1979, Thixotropy- a general review, *J. Non-Newtonian Fluid Mech.* **6**, 1-20.
- Mewis, J., A. J. B. Spaul and J. Helsen, 1975, Structure hysteresis, *Nature* **253**, 618-619.
- Minale, M., P. Moldenaers and J. Mewis, 1999, Transient flow experiments in a model immiscible polymer blend, *J. Rheol.* **43**, 815-827.
- Mobuchon, C., P. J. Carreau and M-C. Heuzey, 2007, Effect of flow history on the structure of a non-polar polymer/clay nanocomposite model system, *Rheol. Acta* **46**, 1045-1056.
- Moldenaers, P., G. G. Fuller and J. Mewis, 1989, Mechanical and optical rheometry of polymer liquid-crystal domain structure, *Macromolecules* **22**, 960-965.
- Pignon, F., A. Magnin and J-M. Piau, 1998, Thixotropic behaviour of clay dispersions: combinations of scattering and rheometric techniques, *J. Rheol.* **42**, 1349-1373.
- Potantin, A., 2004, Thixotropy and rheology of aggregated dispersions with wetting polymer, *J. Rheol.* **48**, 1279-1293.
- Prasad, V., V. Trappe, A. D. Dinsmore, P. N. Segre, L. Cipolletti and D. A. Weitz, 2003, Universal features of the fluid to solid transition for attractive colloidal particles, *Faraday Discuss.* **123**, 1-12.
- Ray, S. S. and M. Okamoto, 2003, Polymer/layered silicate nanocomposites: a review from preparation to processing, *Prog. Polym. Sci.* **28**, 1539-1641.
- Ren, J., B. Casanueva, C. Mitchell and R. Krishnamoorti, 2003, Disorientation kinetics of aligned polymer layered silicate nanocomposites, *Macromolecules* **36**, 4188-4194.
- Solomon, M. J., A. S. Almusallam, K. F. Seefeldt, A. Somwangthanoj and P. Varadan, 2001, Rheology of polypropylene/clay hybrid materials, *Macromolecules* **34**, 1864-1872.
- Trappe, V. and D. A. Weitz, 2000, Scaling of the viscoelasticity of weakly attractive particles, *Phys. Rev. Lett.* **85**, 449-452.
- Vaia, R. and E. Giannelis, 1997, Polymer melt intercalation in organically-modified layered silicates: model predictions and experiment, *Macromolecules* **30**, 8000-8009.
- Vermant, J., S. Ceccia, M. K. Dolgovskij, P. L. Maffettone and C. W. Macosko, 2007, Quantifying dispersion of layered nanocomposites via melt rheology, *J. Rheol.* **51**, 429-450.
- Vinckier, I., J. Mewis and P. Moldenaers, 1997, Stress relaxation as a microstructural probe for immiscible polymer blends, *Rheol. Acta* **36**, 513-523.
- Willenbacher, N., 1996, Unusual thixotropic properties of aqueous dispersions of Laponite RD, *J. Colloid Interface Sci.* **182**, 501-510.
- Wyss, M. M., E. V. Tervoort and L. J. Gauckler, 2005, Mechanics and microstructures of concentrated particle gels, *J. Am. Ceram. Soc.* **88**, 2337-2348.